Structure of a Transient Neutral Histidine Radical in Solution: EPR Continuous-Flow Studies in a Ti^{3+}/EDTA−Fenton System and Density Functional Calculations

Günter Lassmann,*,† Leif A. Eriksson,‡ Friedhelm Lendzian,† and Wolfgang Lubitz†

Max-Volmer-Institute for Biophysical Chemistry and Biochemistry, Technical University of Berlin, D-10623 Berlin, Germany, and Department of Quantum Chemistry, Uppsala University, Box 518, S-75120 Uppsala, Sweden

Received: April 14, 2000; In Final Form: July 25, 2000

Oxidation of histidine by OH* radicals has been studied at room temperature over a large range of pH values in a Ti^{3+} /EDTA/H_2O_2−Fenton system using a special EPR continuous-flow setup. At pH 7 to 8, during fast flow, an EPR spectrum from a new transient histidine radical with a well-resolved hyperfine structure (hfs) has been observed at $g_{iso} = 2.0026$. The hfs changed significantly in the cases of methylene-deuterated histidine in H_2O and of histidine in D_2O. EPR spectral simulations resulted in an assignment of two slightly different splittings of the two methylene protons (1.27 and 1.59 mT); one large splitting from an out-of-plane proton of the imidazole ring (2.47 mT); and splittings of a ring proton (0.99 mT), a NH (or OH) proton (0.14 mT), and two ring nitrogens (0.27 and 0.11 mT). The large proton-splitting indicates an addition of an OH* radical to the neutral imidazole ring. Such an addition of an OH* radical was already observed for the histidine cation radical in a Ti^{3+}/H_2O_2 Fenton system at pH 2.[1] Density functional theory (DFT) calculations of hyperfine coupling constants were performed at the PCM/B3LYP/6-311G(2df,p) level for three isomeric forms of a histidine model (4-ethyl imidazole) in which an OH* radical is added to different positions (C2, C4, and C5) of the neutral imidazole ring. Theoretical hyperfine data are in excellent agreement with the experiment and clearly support an assignment to a neutral histidine radical formed by addition of an OH* radical at the C5 position of the imidazole ring. Extensive studies of histidine oxidation in a Ti^{3+}/EDTA−Fenton system, at acidic pH as well as at neutral and basic pH values, have advanced our understanding of the Fenton chemistry of histidine and the electronic structure of involved paramagnetic species. The pH profile of the formation of histidine OH-addition radicals shows that the cation radical dominates at pH 2 to 4, and the neutral radical at pH 5 to 9. At pH ≥7, in the presence of histidine, a titanium complex with $g_{iso} = 1.9632$ and a significant hfs from naturally occurring ^{47}Ti and ^{49}Ti nuclei with $a_{iso}(Ti) = 1.54$ mT has been observed. This complex, which dominates at pH 9 to 10, is also visible in the absence of H_2O_2 and without flow, and is thus assigned to a stable mixed-ligand Ti^{3+} complex containing EDTA and histidine. This is the first communication on a neutral histidine radical with a complete set of hyperfine coupling constants derived by EPR as well as by DFT calculations.

1. Introduction

Histidine is frequently encountered as a ligand in metalloproteins and radical enzymes. In electron-transfer processes and biological redox reactions, including oxidative stress, histidine radicals may be formed as transient intermediates. In photosystem II, oxidized histidine radicals have been postulated from UV−vis data, but an electron paramagnetic resonance (EPR) identification with hfs data was not given (see ref 1 and refs 13−16 cited therein).

In metalloenzymes and radical enzymes, however, protein-associated histidine radicals have not yet been identified by standard EPR techniques, as has been done for tyrosine radicals[2−5] and tryptophan radicals.[6−9] Therefore, EPR spectroscopic studies of histidine radicals in protein-free model systems in an aqueous medium under oxidative conditions are required. We have started systematic EPR investigations of the electronic structure of histidine radicals formed in the Ti^{3+}/H_2O_2−Fenton system at pH 2. The resulting transient histidine *cation* radical, which was generated in a fast EPR continuous-flow system by oxidative attack of an OH* radical on histidine, has recently been described.[1]

In the present paper, we have extended these EPR studies by means of a modified Ti^{3+}−Fenton system containing ethylenediaminetetraacetic acid (EDTA).[10,11] Our aim is to study histidine radicals at physiologically interesting neutral pH values. At pH 7 to 8, another transient radical with a well-resolved hyperfine structure (hfs) is thereby detected and assigned to a *neutral* histidine radical. Density functional theory (DFT) calculations of histidine models (4-ethyl imidazole) indicate that the observed radical is formed by addition of an OH* radical to position C5 of the imidazole ring. Furthermore, at basic pH, a paramagnetic Ti^{3+}−EDTA/histidine complex with significant Ti hfs is observed in solution.

2. Materials and Methods

L-Histidine, $TiCl_3$, and H_2O_2 were obtained from Fluka; DL-α,β,β-d3-histidine was from CDN Isotopes, Quebec, Canada. EDTA was purchased from Sigma. D_2O (99.9% D) was obtained

* To whom correspondence should be addressed.
† Technical University of Berlin.
‡ Uppsala University.

10.1021/jp001437w CCC: $19.00
Published on Web 09/20/2000

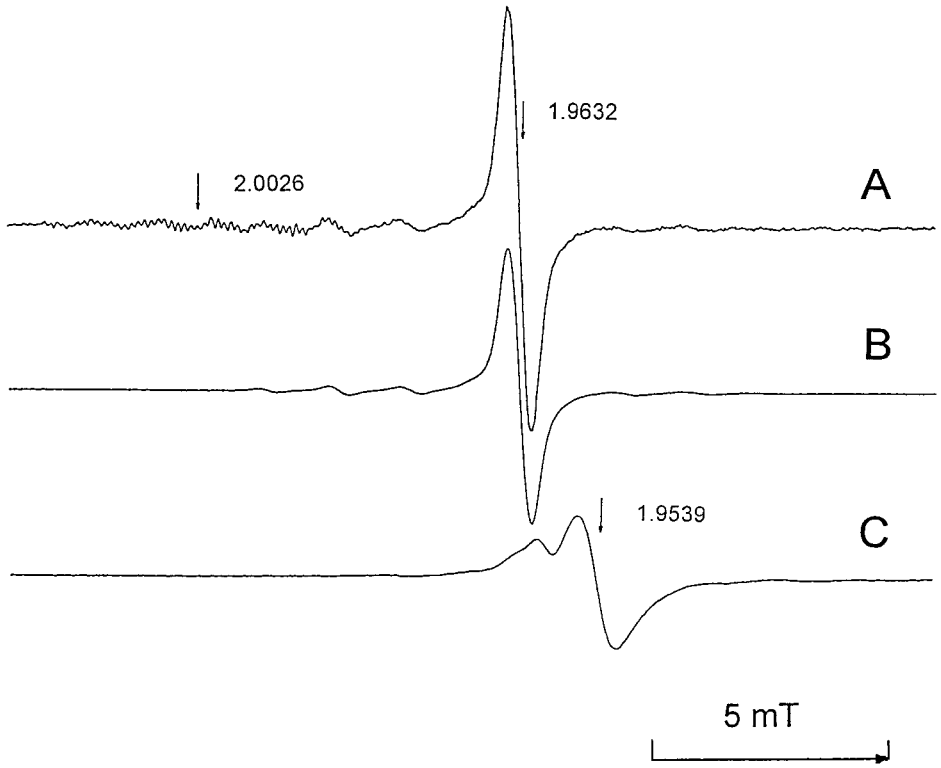

Figure 1. EPR spectra of paramagnetic species in solution formed upon oxidation of histidine in a Ti^{3+}/EDTA/H_2O_2−Fenton system using a continuous-flow setup. EPR parameters: MW power, 1 mW; modulation, 0.05 mT; sweep time, 41 s; time constant, 41 ms. (A) Oxidized histidine, fast flow (flow rate 24 mL/min); pH 7. Reactant I, Ti^{3+} (14 mM)/EDTA (14 mM)/His (80 mM) + reactant II, H_2O_2 (80 mM)/His (80 mM). (B) Control: Without H_2O_2, no flow, pH 7. Reactant I, Ti^{3+} (14 mM) + reactant II, EDTA (14 mM)/His (80 mM). (C) Control: Without histidine and without H_2O_2, no flow, pH 9. Reactant I, Ti^{3+} (14 mM) + reactant II, EDTA (14 mM).

from Campro. In studies with D_2O as solvent, the addition of H_2O_2 and acidic $TiCl_3$ contributes together to 1.5% H in the assay.

Histidine was oxidized by OH* radicals which were generated in a Ti^{3+}/EDTA/H_2O_2−Fenton system in the pH range from 2 to 10. EDTA in equimolar amounts as Ti^{3+} was used to prevent precipitation of $Ti(OH)_3$ at pH >2. For EPR studies, the two reactants (reactant I, containing histidine/H_2O_2, and reactant II, containing histidine/Ti^{3+}/EDTA) are driven by a syringe pump through the Y-mixer (1:1 mixing) and the dielectric resonator (EPR-active volume: 2 μL) of the EPR mixing resonator (ER-4117D-MVT, Bruker), which was especially designed for continuous-flow studies with low reactant consumption. EPR spectra of transient species were recorded during a fast flow (flow rate up to 24 mL/min) by an EPR spectrometer (ESP 300E, Bruker). For more experimental details of this technique, see ref 1. Concentrations of reactants and flow conditions, optimized to obtain a sufficient steady-state concentration of histidine radicals, are given in the legends of Figures 1−3. Potassium peroxylamine disulfonate (Fremy's salt; Sigma) with $g_{iso} = 2.0054 \pm 0.0001$ (measured with an NMR gaussmeter) was taken as *g*-standard for aqueous solutions using the same sample geometry in the dielectric flow resonator. Simulation of EPR spectra was performed using a computer program which allows a fit of the calculated isotropic hyperfine (hf) spectrum optimized to the experimental one.[8,12]

3. Results

3.1. EPR Data of Species upon Oxidation of Histidine in a Ti^{3+}/EDTA−Fenton System. *3.1.1. Transient Histidine Radical in Aqueous Solution at Neutral pH.* Histidine was oxidized by OH* radicals in a modified Ti^{3+}/H_2O_2−Fenton system, which contains equimolar amounts of Ti and EDTA complexing the metal ion and allows us to observe the reaction in neutral and alkaline pH values.[10,11]

After rapid mixing of Ti^{3+}/EDTA/histidine with H_2O_2/histidine (1:1) at pH 7, a complex EPR spectrum with about 50 resolved lines centered at $g_{iso} = 2.0026$ was observed during a continuous fast flow through the dielectric EPR resonator (Figure 1A). In the spectrum's high-field part, satellite lines from a strong singlet EPR line are superimposed; these are also present without flow (Figure 1B). The complex EPR spectrum appears only at fast flow rates (24 mL/min)(compare Figure 1A with 1B) and in the presense of histidine (compare Figure 1A with 1C). The multiline spectrum in Figure 1A therefore belongs to a transient species. The strong singlet line in Figure 1B represents a stable species with a *g* factor of $g_{iso} = 1.9632$ and a hyperfine structure from satellite lines of natural abundant Ti-isotopes with nonzero nuclear spin; both of these features are characteristic for Ti^{3+} complexes[13−15] (see section 4.3). The EPR spectrum of the stable Ti^{3+} complex (Figure 1B) has been subtracted from the spectrum in Figure 1A for spectral analysis; the difference spectrum is shown in Figure 2A.

The complex EPR spectrum of the transient species from histidine in H_2O (Figure 2A) consists of six groups of lines with an intensity ratio of about 1:3:4:4:3:1. Each group subsplits into eight lines with an intensity ratio of 1:2:3:3:3:3:2:1, best visible in the outermost groups. The EPR spectrum of α,β,β-d3-deuterated histidine in H_2O recorded under comparable conditions (Figure 2B) differs significantly from that of protonated histidine in H_2O, changing the ground pattern to 1:1:1:1. In case of histidine in D_2O, the ground sextet remained, but the subsplitting is changed into a septet with an intensity ratio of 1:1:2:1:2:1:1 as visible in the outermost groups (Figure 2C).

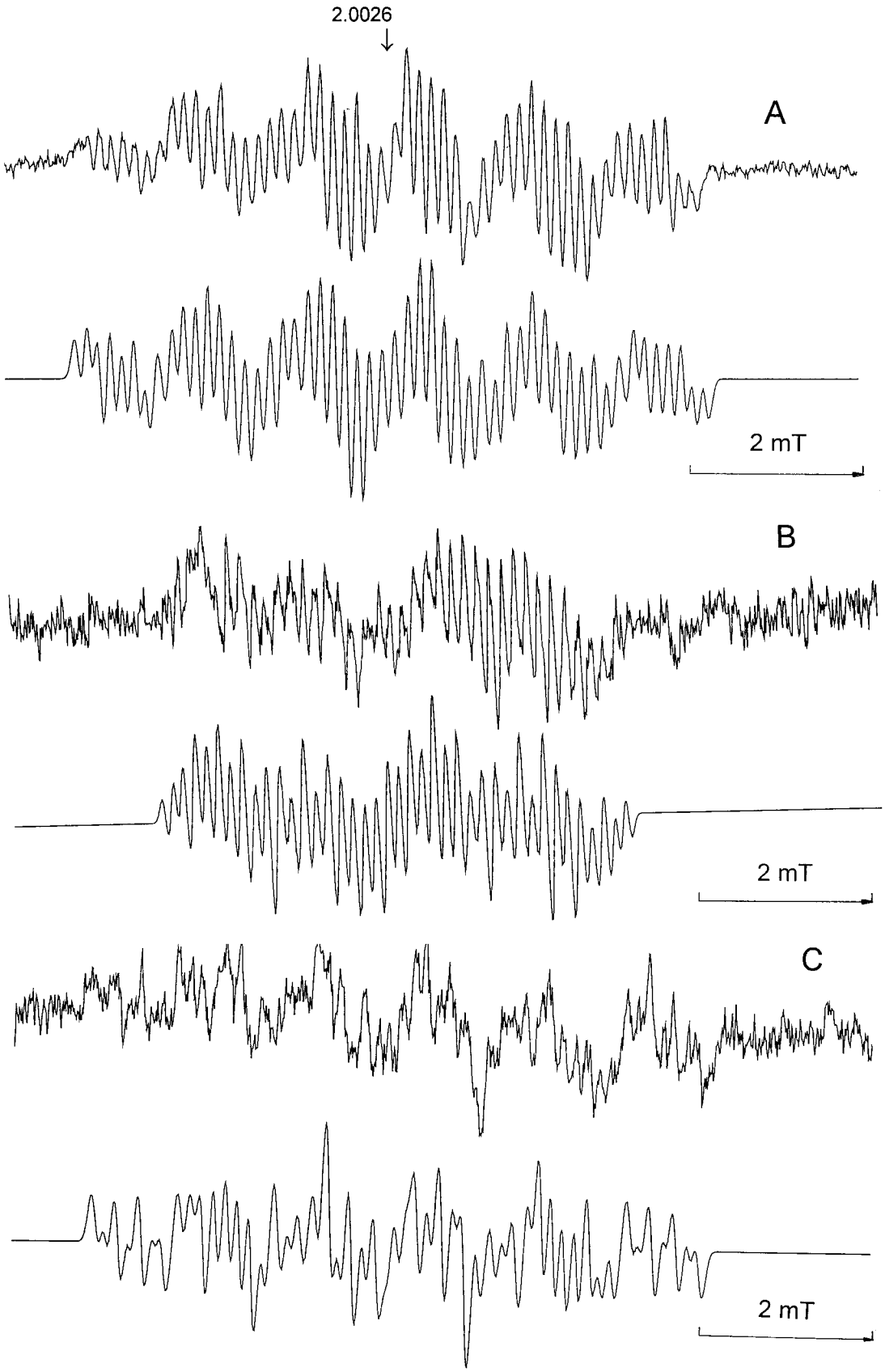

Figure 2. EPR spectra of transient neutral histidine radicals in solution formed upon oxidation of histidine in a Ti^{3+}/EDTA/H_2O_2−Fenton system at pH 7, recorded under fast continuous flow (flow rate 24 mL/min). Superimposed low-field satellite EPR lines from a Ti^{3+} complex (see Figure 1B) have been subtracted. Simulated spectra are below the experimental ones (see text). EPR parameters: MW power, 1 mW; modulation, 0.05 mT; sweep time, 41 s (A, C), 20 s (B); time constant, 41 ms (A, C), 20 ms (B); 21 scans (A), 4 scans (B), 10 scans (C). (A) Histidine in H_2O: Reactant I, Ti^{3+} (14 mM)/EDTA (14 mM)/His (80 mM) + reactant II, H_2O_2 (80 mM)/His (80 mM). (B) α,β,β-d3-Histidine in H_2O: Reactant I, Ti^{3+} (14 mM)/EDTA (14 mM)/His (40 mM) + reactant II, H_2O_2 (80 mM). (C) Histidine in D_2O: Reactant I, Ti^{3+} (14 mM)/EDTA (14 mM)/His (80 mM) + reactant II, H_2O_2 (80 mM)/His (80 mM).

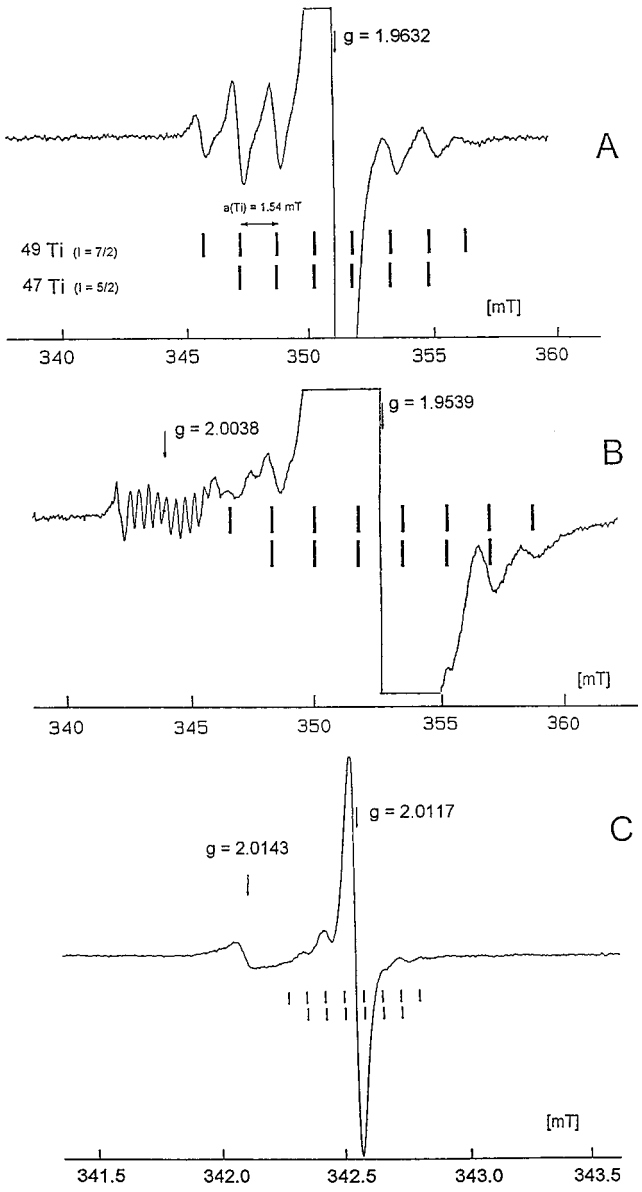

Figure 3. Ti hyperfine structure of titanium complexes in solution (bars indicate the position of Ti hfs lines). (A) EPR spectrum of a Ti^{3+}/EDTA/histidine complex at pH 7; no flow, no H_2O_2 (see also Figure 1B). Reactant I, Ti^{3+} (14 MM) + reactant II, EDTA (14 mM)/His (80 mM). EPR parameters: MW power, 1 mW; modulation, 0.05 mT; sweep time, 41 s; time constant, 41 ms; 2 scans. (B) EPR spectrum of a Ti^{3+}−EDTA complex at pH 10 (without histidine; intense line with satellites from Ti hfs at high field [see also Figure 1C], and a transient EDTA radical at low field). Reactant I, Ti^{3+} (14 mM)/EDTA (14 mM) + reactant II, H_2O_2 (80 mM). Flow rate 24 mL/min. EPR parameters: MW power, 3 mW; modulation, 0.1 mT; sweep time, 41 s; time constant, 41 ms; 2 scans. (C) EPR spectrum of a Ti^{4+}−O_2* adduct formed in the Ti^{3+}/EDTA/H_2O_2−Fenton system at pH 7 (with excess H_2O_2 and without histidine). Flow rate 20 mL/min. Reactant I, Ti^{3+} (14 mM)/EDTA (14 mM) + Reactant II, H_2O_2 (500 mM). EPR parameters: MW power, 0.3 mW; modulation, 0.03 mT; sweep time, 21 s; time constant, 20 ms; 24 scans.

The general analysis of the EPR hyperfine pattern shows that the ground sextet in the spectrum from histidine in H_2O originates from three nearly equivalent protons (1.0−1.5 mT) and another proton with an hf coupling constant that is twice as large. Two of the three major couplings are absent in the spectrum of the $\beta\beta$-deuterated histidine; these couplings must arise from the two β protons. The octet subsplitting of each sextet group in the spectrum from histidine in H_2O is caused

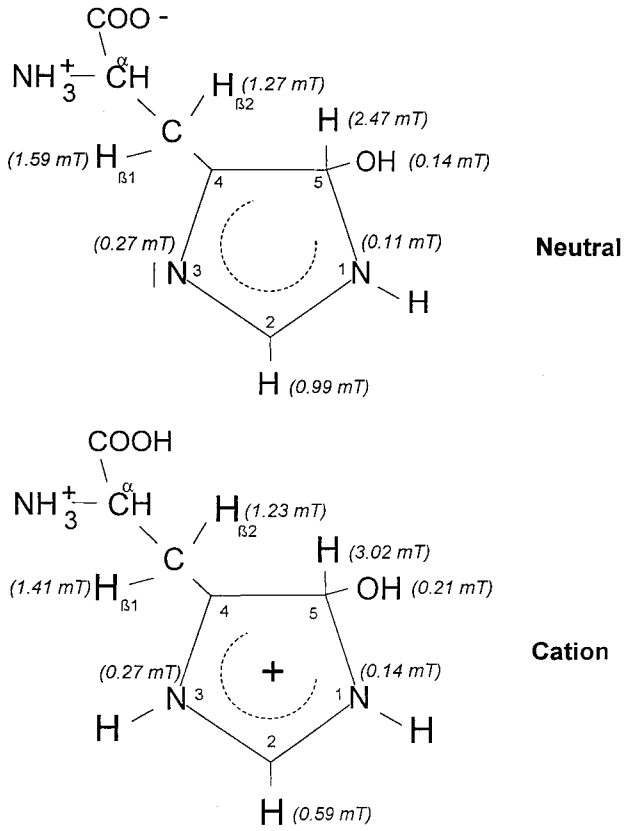

Figure 4. *Experimental* isotropic hyperfine coupling constants of histidine radicals in solution (absolute values of hfcc's are given in italic letters next to the corresponding nuclei). Top, neutral histidine OH-addition radical (this paper). Bottom, cationic histidine OH-addition radical (from ref 1).

by one nitrogen and one proton (about 0.13 mT each) and another nitrogen with a splitting twice as large. The EPR spectrum from histidine in D_2O shows that this small proton splitting is missing; it belongs therefore to a dissociable NH or OH proton. The simulation of the three EPR spectra shown in Figure 2A−C is the optimized fit to the corresponding experimental ones, and results in the following hyperfine coupling constants (hfcc's) in millitesla:

	H_a	H_b	H_c	H_d	H_e	N_a	N_b
His (H_2O)	2.47	1.59	1.27	0.99	0.14	0.27	0.11
His (D_2O)	2.47	1.56	1.15	0.99	0.022 (D)	0.27	0.11
$\beta\beta$-d-His (H_2O)	2.47	0.258 (D)	0.207 (D)	0.99	0.14	0.27	0.11

The simulation of the histidine radical in H_2O (Figure 2A) fits well. The S/N ratio of the spectra from the two deuterated samples (Figure 2B,C) is less because it allows, by economical reasons, only a limited number of accumulations. Even so, comparison with the simulated spectra confirms for $\beta\beta$-deuterated histidine the loss of the two large splittings of spin 1/2 nuclei, and for protonated histidine in D_2O the disappearance of a small coupling from a spin 1/2 nucleus. The assignment of the hfc's to the corresponding nuclei of the neutral histidine radical is discussed in section 4.1.1 and shown in Figure 4 (top).

The formation of the neutral histidine radical in the Ti^{3+}/EDTA−Fenton system at pH 7 is optimal at an equimolar concentration of Ti^{3+} and EDTA (14 mM), a high concentration of histidine (80 mM), and a moderate concentration of hydrogen peroxide (80 mM). The steady-state concentration of the transient histidine radical at the optimum pH of 7 upon rapid flow is about 50 μM; it was estimated by spectral integration

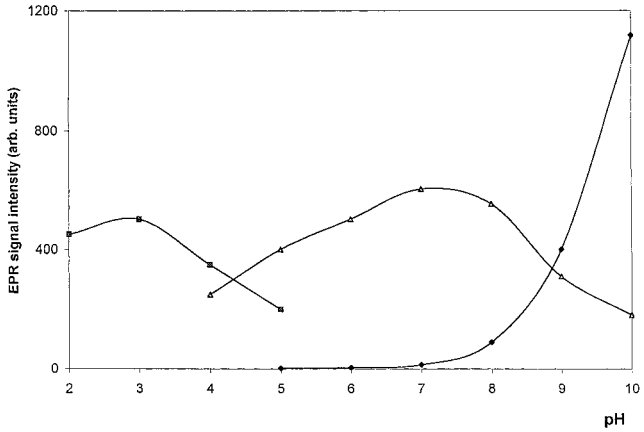

Figure 5. Relative EPR amplitudes of paramagnetic species formed upon oxidation of histidine in a Ti^{3+}/EDTA/H_2O_2−Fenton system as a function of pH. (■) histidine OH-addition cation radical; (△), histidine OH-addition neutral radical; (●), Ti^{3+}−EDTA/histidine complex (amplitudes scaled down by a factor of 50).

and comparison with a stable nitroxide radical standard of known concentration. Lower histidine concentrations and/or higher H_2O_2 concentrations (500 mM) lead to less intensity of the transient complex EPR spectrum from the neutral histidine radical. Instead, a transient EPR singlet at $g = 2.0151$ with a line width of 0.2 mT appears (visible in the low-field part of Figure 2B). This EPR line has also been observed at pH 2 (without EDTA) and was assigned earlier to a histidine peroxy radical.[1]

3.1.2. Stable Ti^{3+}−Histidine/EDTA Complex at Alkaline pH. Under conditions of optimal generation of the neutral histidine radical in the Ti^{3+}/EDTA−Fenton system, the last two high-field groups of the sextet EPR pattern of the neutral histidine radical are superimposed by satellite lines from an intense EPR singlet at $g_{iso} = 1.9632$ (Figure 1A,B). This EPR spectrum appears only in the presence of histidine and increases with increasing histidine concentration. The satellite lines on both sides of the singlet (Figure 3A) originate from hyperfine lines of the isotopes ^{49}Ti and ^{47}Ti with $a_{iso}(Ti) = 1.54$ mT; these will be discussed in section 4.3. The Ti hfs and the *g* factor 1.9632 identify the singlet as a paramagnetic Ti^{3+}-centered complex. The concentration of this Ti^{3+} complex increases considerably at pH 9 to 10 (see Figure 5). Because it is also visible in absence of hydrogen peroxide and without flow (Figure 1B), this rather stable species does not originate from a reaction with OH* radicals. In the presence of H_2O_2, however, it is short-lived because paramagnetic Ti^{3+} is oxidized to diamagnetic Ti^{4+}.

3.2. EPR Data of Titanium Complexes without Histidine. *3.2.1. Stable Ti^{3+}−EDTA Complex at pH 9 to 10.* To separate superimposed EPR spectra of other species from histidine radicals in the complex mixture of the Fenton system, control experiments without histidine were performed. In the absence of histidine and H_2O_2, and at alkaline solution (pH 9 to 10) of equimolar concentrations of Ti^{3+} and EDTA (14 mM), a stable EPR single line at $g = 1.9539$ (line width $\Delta H = 0.9$ mT) appears (Figure 1C). This EPR signal has been observed earlier and was assigned to a stable metal chelate complex of the paramagnetic Ti^{3+} ion with EDTA;[10,11] a smaller EPR line at $g = 1.9601$ (low-field shoulder) may be due to a Ti^{3+} complex with a modified ligand coordination, eventually partially protonated EDTA.[16] External satellite lines from natural abundant Ti isotopes ^{47}Ti and ^{49}Ti, with $a_{iso}(Ti) = 1.70$ mT (see below), are also resolved on the wings of the central line and are better

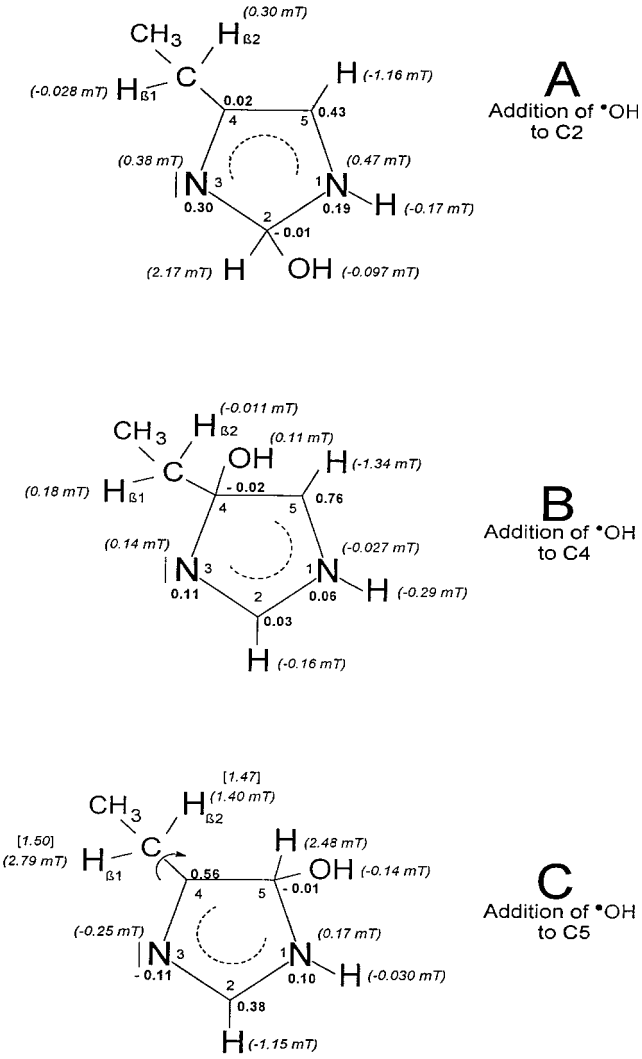

Figure 6. DFT data* of hyperfine coupling constants and spin densities of three different neutral OH-addition radicals of the histidine model 4-ethyl imidazole (see text for details). * is based on PCM/B3LYP/6-311G(2df,p)//B3LYP/6-311G(d,p) calculations (hfcc's, in italics, and spin densities, in bold, are given next to the corresponding nuclei). *β*-hfcc: ( ), static values; [ ], averaged values of freely rotating side chain.

visible in Figure 3B. In the presence of histidine, this Ti^{3+}−EDTA complex is converted to the complex at $g = 1.9632$ as discussed in section 3.1.2. After addition of H_2O_2 to the Ti^{3+}−EDTA complex (without histidine) and with flow at pH 10, the Ti^{3+}−EDTA complex at 1.9539 is short-lived because of an oxidation of the paramagnetic Ti^{3+} to the diamagnetic Ti^{4+}. In addition, a spectrum of an EDTA radical,[10] formed by an attack of an OH* radical, appears at $g = 2.0038$ (Figure 3B). It is essential to note, however, that at neutral pH and in the presence of an excess of histidine (80 mM), histidine radicals are the dominating species, and EDTA radicals−which are superimposed on the EPR spectrum of histidine radicals−are no longer formed by OH* attack (Figure 1A).

3.2.2. Transient Ti^{4+} Complex at Neutral pH. In the absence of the substrate histidine, and with excess hydrogen peroxide, the reaction of Ti^{3+}/EDTA with H_2O_2 at pH 7 yields two narrow, transient singlet EPR signals (see Figure 3C), one weak at $g_1 = 2.0143$ (line width ΔH: 0.08 mT) and one strong at $g_2 = 2.0117$ (ΔH: 0.06 mT); both of them were previously observed at pH 2 without EDTA.[17]

The stronger transient species exhibits Ti hfs in the wings; its intensity has been optimized for a detection of the ^{47}Ti and

TABLE 1: EPR Data of Ti Complexes in Liquid Solution

	$*Ti^{3+}$/EDTA/His in H_2O stable, pH 7−10	$*Ti^{3+}$/EDTA in H_2O stable, pH 9−10	$Ti^{4+}-O_2*$ in H_2O transient, pH 7	$*Ti^{3+}/CH_3O$[d] in methanol
g_{iso}[a]	1.9632	1.9539	2.0117	1.9532
g_1[b]	1.9925	1.9875		
g_2[b]	1.9573	1.9577		
g_3[b]	1.9450	1.9419		
ΔH[a,c]	0.5 mT	0.8 mT	0.06 mT	
a_{iso}(Ti)[a]	1.54 mT	1.70 mT	0.08 mT	1.82 mT

[a] Measured in liquid state. [b] Measured in frozen state at 77 K at *X*-band. [c] Central component measured between extrema of 1st derivative. [d] From ref 14.

^{49}Ti satellites, for comparison with the Ti hfs of the two stable paramagnetic Ti^{3+} complexes discussed above. The observed $a_{iso}(Ti) = 0.08$ mT of the species with $g = 2.0117$ (Figure 3C) is much less than those observed for the two Ti^{3+} complexes (Figure 3A,B; Table 1). The origin and nature of this Ti^{4+} complex is discussed later, in section 4.3.

3.3. DFT Calculations of Hyperfine Coupling Constants of Neutral 4-Ethyl Imidazole Radicals. *3.3.1. Theoretical Approach.* For the DFT calculations of histidine radicals, 4-ethyl imidazole was chosen as a model because of its ability to mimic the two β-protons. The amino and carboxylic groups of the amino acid carry negligible spin density and were hence neglected for computational reasons. The three possible OH-radical adducts to 4-ethyl imidazole (at positions C2, C4, and C5) were fully geometry optimized at the hybrid HF−DFT level B3LYP,[18] using a valence triple-ζ basis set, 6-311G(d,p).[19] Frequency calculations were performed to verify that the systems were in local minima and to generate zero-point vibrational energies (ZPE). Subsequently, single-point calculations were carried out using the larger 6-311G(2df,p) basis set, including a polarized continuum model (PCM)[20,21] with the aim to mimic the effect of the surrounding water. This combination of methods has previously shown to yield radical hyperfine properties of very high accuracy.[22−24]

Once the correct radical adduct had been identified, rotational averaging was carried out for the (free) rotation of the imidazole head against the side-chain tail (see Figure 6C) by moving the rotational angle in steps of 15° and reoptimizing all other geometric parameters in each step. Once again, these rotational B3LYP/6-311G(d,p) optimizations were followed by single-point PCM/B3LYP/6-311G(2df,p) calculations. All calculations were performed using the GAUSSIAN98 program.[25]

3.3.2. Relative Stabilities and hfc's of Optimized OH Adducts. The OH adducts of neutral imidazole, and the corresponding mechanisms of addition reaction, have previously been investigated in great detail using polarized continuum models and spin-projected MP2 or B3LYP levels of theory.[24] It was concluded that the most thermodynamically stable product is the C2−OH form, and that the experimentally favored C5 adduct is a result of the lower transition barrier to addition. This could in turn be explained in terms of the anomeric effects for the different transition structures, on the basis of a detailed analysis of the natural bond orders (NBOs).

The computed PCM/B3LYP/6-311G(2df,p) energies of the hydroxyl adducts to 4-ethyl imidazole in this paper agree with the previously reported energetic stabilities, although the PCM model and ZPE effects give an energy difference between C2−OH and C5−OH of less than 0.1 kcal/mol. The C4−OH adduct is, however, still more than 10 kcal/mol less stable than the other two (13.2 kcal/mol in the present case). The difference in relative stabilities of the C2−OH versus the C5−OH adduct obtained in the present study compared to the previous work[24] can be explained in terms of both a different solvent model (PCM versus SCI−PCM) and the use of a larger model for the calculations (4-ethyl imidazole versus imidazole).

In Figure 6 the hfcc's (in italic) and spin densities (in bold) at the optimized geometries of the three hydroxy 4-ethyl imidazolyl radicals are displayed at the corresponding nuclei of the molecule. For the C2−OH adduct (Figure 6A), the unpaired spin is distributed mainly among *three* centers, the two nitrogens and C5, which results in relatively large hfcc's of the nitrogens and the H5 α-proton. In addition, the out-of-plane H2 proton attains a large positive coupling due to hyperconjugative interaction with the π-type singly occupied molecular orbital (SOMO). The β-couplings are fairly small, because carbon C4 carries very little unpaired spin density. In the C5−OH adduct (Figure 6C), however, there are *two* distinct spin centers, at positions C2 and C4. As a consequence, the ^{14}N hfcc's are only about half of those seen for C2−OH, and the two β-couplings are considerably larger. In the C4−OH adduct (Figure 6B), there is only *one* primary radical center, at position C5, and no large positive ring-proton hyperfine coupling constant because no proton is attached to the addition site.

3.3.3. Rotational Averaging. Because the molecules are present in aqueous solution and the experiments are performed at room temperature, it is reasonable to assume that the imidazole head is allowed to make rapid rotational fluctuations relative to the tail. The orientation of the methylene protons relative to the ring plane can be expected to have a strong influence on the resulting β-proton hfcc's, given that the SOMO is of π-type. In the previous work on cationic histidine radicals,[1] assumption of a full rotational averaging was found to be necessary to understand the observed, nearly equivalent β-couplings of the C5−OH adduct. In the present system, the full rotational averages are 1.50 and 1.47 mT for the two β-protons (Figure 6C, rectangular brackets).

4. Discussion

4.1. Electronic Structure of the Neutral Histidine OH-Addition Radical in Aqueous Medium. *4.1.1. Assignment of the Hyperfine Data to Radical Structure.* According to the p$K = 6.5$ for histidine[26], it is expected that at pH 7 the imidazole ring is in the neutral state with one deprotonated and one protonated nitrogen, and the formed radical may thus be assumed to be derived from *neutral* histidine. The largest doublet splitting of 2.47 mT undoubtedly originates from a proton being out-of-plane of the imidazole ring, which occurs when a radical (here OH*) is added to the imidazole ring. This unusually large splitting gives strict evidence for the *type* of formed radical, namely an OH-addition type radical of neutral histidine. An analogous type of radical has already been observed for the *cationic* histidine radical formed by a Ti^{3+}/Fenton oxidation at pH 2.[1]

Two of the three other larger proton-splittings belong to the two β-protons of histidine, which are replaced in α,β,β-d3-

histidine by deuterium. The EPR spectrum of the $\beta\beta$-deuterated histidine radical (Figure 2B) yields an unambiguous assignment of these proton hfcc's. Beside the largest proton splitting of the out-of-plane proton, clearly visible as two major spectral components, one proton subsplitting of each of the two components can be seen. From the three options, 0.99 mT, 1.27 mT, or 1.59 mT, only the 0.99 mT splitting fits in the simulation for this subsplitting in Figure 2B. Because the two other proton-splittings (1.58 mT and 1.27 mT) observed in protonated histidine are missing in the case of the $\beta\beta$-deuterated histidine, they must originate from the two β-protons. The 0.99 mT proton-splitting is therefore assigned to an imidazole ring proton, as shown below from DFT data, to position C2. According to the calculations the sign of this hfcc is negative. As shown by the missing 0.14 mT proton-splitting in D_2O (Figure 2C), this splitting arises from an exchangeable proton of the NH or the added OH group (Figure 4). A comparison with the DFT data for these protons (Figure 6C) supports the assignment to an OH proton. The assignment of the *experimentally* determined hfc's to the electronic structure of the neutral histidine OH-addition radical is shown in Figure 4 (in italic at the corresponding nuclei). The assignment based on a comparison of the hfc's of three possible positions of addition of OH* to C2, C4, and C5 of the imidazole ring, with DFT-calculated hfcc's on model radicals of 4-ethyl imidazole.

4.1.2. Comparison of Hyperfine Splittings from EPR Experiment and DFT Calculations. The computed hyperfine splittings for the 4-ethyl imidazole radicals, the model for neutral histidine radicals, are given in Figures 6A (C2−OH), 6B (C4−OH), and 6C (C5−OH). Comparing the theoretical values with the experimentally determined hfcc's from the EPR measurements (see section 3.1.1 and Figure 4), it is obvious that OH additions to C5 yield the best agreement with the EPR data. As can be seen, the agreement is perfect for all atoms when rotational averaging is assumed for the β-protons as described above. C4 addition can immediately be ruled out because it lacks the large proton-splitting of 2.47 mT. In the case of OH addition at C2, the theoretical ^{14}N-splittings are too large in comparison to the experimental ones, and also the H2 and H(O) couplings deviate too much to be fully satisfactory.

In liquid state, methylene β-protons undergo rapid rotational fluctuations which usually lead to equal β-couplings. In the neutral histidine radical, however, we observe a slight inequivalence, both experimentally and in the calculations. Such a behavior has also been observed previously in the liquid state of radicals with a tetrahedral distorted chiral C-atom adjacent to the methylene group, e.g., in tyrosine radicals[27] and in various nitromethane radicals with chiralic substituents (but not with nonchiral substituents).[28] To account for rotational averaging of β-proton couplings, the head-to-tail rotation (see sections 3.3.1 and 3.3.3) was assumed to be completely free, and hence an average was computed as outlined above. The average theoretical hfc's, 1.50 and 1.47 mT, display a slight asymmetry as noted experimentally, and is also in reasonable agreement with the experimental hfc's of 1.59 and 1.27 mT.

An interesting feature of the conformation of the two β-protons came out in the experiments with D_2O. Although the spectrum simulation fits well for the two external groups, the central part of the spectrum could only be simulated assuming two β-proton hfcc's (1.56 and 1.15 mT) which deviate slightly from the case in H_2O (see section 3.1.1). This may be understood as a slightly changed average value of a_{iso} (changed theta angles) due to the heavier $-^{+}ND_3$ group of histidine in D_2O at pH 7.

Explicitly including solvent molecules, and using a full zwitterionic histidine model, or computing a Boltzmann distribution of hfcc's as functions of relative (rotational) energy in DFT calculations, might improve the fit even further. The present data set, however, is considered sufficiently accurate to positively identify the observed radical as the C5−OH adduct to histidine.

It is interesting to note that the hfcc's of the neutral imidazole radical obtained by in situ radiolysis in liquid state at pH 9−10 and subsequent OH addition (also at C5)[29] are very similar to those observed here for the neutral histidine radical generated by the Fenton reaction, as well as to the DFT data.[24]

4.2. Comparison of the Electronic Structures of the Neutral and the Cationic Histidine OH-Addition Radical. The experimentally determined electronic structures of the neutral histidine OH-addition radical given in this paper (Figure 4A, top), and the corresponding cationic system (from ref 1) (Figure 4B, bottom), albeit quite similar, do exhibit some distinct differences. Both types are OH-addition radicals at position C5 of the imidazole ring, but in the neutral radical the large splitting of the out-of-plane ring proton at C5 (2.47 mT) is smaller than in the charged radical (3.02 mT). The largest difference in the electronic structure of the charged and the neutral radical, however, is the spin density at C2. The hf coupling of the ring proton at position C2 in the neutral histidine radical (0.99 mT) is significantly larger than in the charged radical (0.59 mT) (absolute values).

The two β-proton couplings in the neutral OH-addition radical (1.27 mT and 1.59 mT) are only slightly larger than those of the cationic one (1.23 mT and 1.41 mT).

4.3. Titanium Complexes in Solution. Ti^{3+} has one 3d electron with $S = 1/2$, and its complexes in solution exhibit typical isotropic g values below 2.[13] Satellites from the hfs of the two naturally occurring magnetic Ti isotopes ^{47}Ti and ^{49}Ti were observed from Ti^{3+} complexes in the liquid phase[10,14,16,17] and in single crystals;[15] these are resolved if the line width is small compared with the hf splitting. Nuclear spin and natural abundance are $I = 5/2$ and 7.28% for ^{47}Ti, and $I = 7/2$ and 5.51% for ^{49}Ti. Both isotopes have almost identical gyromagnetic ratios,[30] which leads to the same hf-splittings and a superposition of the sextet from ^{47}Ti and the octet from ^{49}Ti. The relative intensities of the two outermost satellite lines are 0.7% and 1.9% of the central line (see stick diagram in Figure 3) and are best resolved in Figure 3A. As is visible in Figure 3, the high-field satellites are slighly broader than the low-field ones, which is explained by an m_I-dependence of the line width.[14]

The two stable Ti^{3+} complexes observed at pH 7−10 show distinctly different isotropic g-values, line width, and Ti hyperfine splittings (Table 1), which suggests a different ligand structure and different spin density at the Ti nucleus.

Because of the spectroscopic differences of the two Ti^{3+} complexes—a(Ti) = 1.54 mT and $g = 1.9632$ for the Ti^{3+}−EDTA/histidine complex, and a(Ti) = 1.70 mT and $g = 1.9539$ for the Ti^{3+}/EDTA complex (Table 1)—it is reasonable to assume that histidine is involved in the ligand sphere of the Ti^{3+} complex with $g = 1.9632$ in Figure 3A. This assumption is further supported by our observation that the Ti complex at $g = 1.9632$ appears only in the presence of histidine, and its intensity increases with increasing stoichiometry relative to EDTA (data not shown). Therefore, this line is assumed to originate from a ternary Ti^{3+}/EDTA/His complex rather than a modified ligation (coordination) of the Ti^{3+}/EDTA complex. An EPR line from a modified EDTA ligation was observed in the absence of histidine as a low-field shoulder at $g = 1.9601$

of the Ti^{3+}/EDTA main line ($g = 1.9539$) in Figure 1C; its amplitude is pH-dependent according to different protonations of EDTA ligands.

An EPR spectrum of a Ti complex at $g = 1.963$ has been observed previously in similar studies of Fenton oxidation of aliphatic amino acids using Ti^{3+}/EDTA/H_2O_2. This spectrum was assigned to a paramagnetic Ti^{3+}/EDTA/amino acid mixed ligand complex.[10] In these studies, the EPR spectrum of the paramagnetic Ti^{3+} complex with EDTA *and* aliphatic amino acids was reported to be identical for several amino acids. Because EPR line shape, *g* factor, and Ti hyperfine coupling constants of the Ti^{3+}/EDTA/*histidine* complex (Figures 1B, 3A; Table 1) are almost the same as those reported for ligating aliphatic amino acids,[10] it can be assumed that the amino or the carboxyl group of histidine, rather than an imidazole nitrogen, is the ligating entity.

EPR studies on Ti^{3+} complexes with (CH_3-O^-) ligands in liquid methanolic solution[14] (see Table 1) and with acetylacetonate in single crystals[15] have shown an octahedral ligand structure with a strong axial distortion (*g* tensor: $g_{||} = 2.000$, $g_{\perp} = 1.921$; hfs tensor: $a_{||} = 0.67$ mT, $a_{\perp} = 1.87$ mT) which leads to a long spin−lattice relaxation time and enables an EPR observation of the complex even in the liquid state at room temperature.

At basic pH, the tetra-anion of EDTA is hexadentate and forms octahedral complexes with Ti^{3+}, with $g_{iso} = 1.956$.[16] At neutral pH, one or two of the carboxylates of EDTA may be protonated, allowing a ligation by other available ligands (with $g_{iso} = 1.960$[16]) as, e.g., histidine in the present case. The measured isotropic *g* values for the pure Ti^{3+}−EDTA complex and the EDTA/histidine mixed-ligand complex (Table 1) support this explanation.

To learn about the symmetry of the two Ti^{3+} complexes, we measured the *g* tensor values in frozen solution at 77 K by *X*-band EPR. The values are presented in Table 1 (spectra not shown). As expected for Ti^{3+} complexes with octahedral symmetry with strong axial distortion,[14,15] the observed rhombic *g* tensors of both Ti^{3+} complexes exhibit only a small anisotropy and a tendency to an axial symmetry; the ternary EDTA/histidine complex is slighly more axial than the EDTA complex.

The *g* value 2.0117 of the observed *transient* Ti complex differs completely from those of the two stable paramagnetic Ti^{3+} complexes with EDTA and EDTA/histidine, respectively. Because the *g* factor is characteristic for peroxide radicals,[31] and because of the presence of Ti hfs, the strong EPR line in Figure 3C has been interpreted earlier as an adduct between a peroxy radical and a diamagnetic Ti^{4+} ion ($Ti^{4+}-O_2$*).[17,32] The weaker line at $g = 2.0143$ has also been detected in ref 17 and was attributed to those with a different ligand sphere. $Ti^{4+}-O_2$* is assumed to be formed upon attack of OH* radicals on a Ti^{4+}/H_2O_2 complex in the absence of a substrate.[10] Thus, the disappearance of the single-line spectra of this adduct, in the case of added substrate (histidine), can be understood as competition of the substrate with Ti^{4+}/H_2O_2 for the OH* radicals.[17,32]

The small Ti hf splitting in the $Ti^{4+}-O_2$* adduct is about 20 times less than the corresponding values of the two paramagnetic Ti^{3+} complexes with EDTA and EDTA/histidine ligands, respectively (see Table 1). The isotropic *g* factor of 2.0117 and the easy microwave saturation at room temperature in solution ($P_{1/2}$ about 1 mW in *X*-band) underline that most of the spin density is localized at the oxygens of this "Ti^{4+} peroxy ligand radical". However, a small but significant spin density is delocalized onto the Ti nucleus. This is an example of an oxygen-centered radical in the ligand sphere of a metal complex exhibiting a minor spin density at the diamagnetic metal. Table 1 summarizes isotropic *g* factors as well as ^{47}Ti and ^{49}Ti hyperfine splittings of the three observed titanium complexes.

4.4. Fenton Chemistry of Histidine−Formation of Histidine Radicals by Reaction with Ti^{3+}/EDTA/H_2O_2. The involvement of EDTA in the Ti^{3+}−Fenton system allowed us to extend EPR spectroscopic studies of transient histidine radicals upon oxidation by OH radicals from acidic pH 2[1] to the full pH range from pH 2 to 10. As we have shown in this paper, the redox behavior of the titanium ion in the Fenton system is not hampered by the EDTA chelation. The pH dependence of the relative intensities of paramagnetic species formed upon Fenton oxidation of histidine is shown in Figure 5. The cationic histidine OH-addition radical analyzed in ref 1, whose EPR spectrum is identical in Ti^{3+}−Fenton and in Ti^{3+}/EDTA−Fenton, is dominant at pH 2 to 4. The neutral histidine OH-addition radical—as studied in this paper—occurs at pH 5 to 9, with maximum intensity at pH 7−8. The pH dependence of these differently charged histidine radicals is in accordance with the p*K* 6.5 of the imidazole group. At pH ≥7, a paramagnetic Ti^{3+} complex with mixed ligands of EDTA and histidine appears. Its yield increases from pH 7 to pH 10 by about 2 orders of magnitude. Thus, the Fenton chemistry of histidine has been studied for a large range of pH values, and it involves the elucidation of the electronic structure of both the cationic *and* the neutral histidine radicals.

Titanium-associated peroxy radicals ($Ti^{4+}-O_2$*) have been discussed as oxidizing agents in the Ti−Fenton system as alternatives to OH* radicals.[10] Such species have most likely been observed by EPR as transient intermediates in the absence of histidine in this paper. However, the determined electronic structure of both histidine radicals, the cationic one at pH 2 as well as the neutral one at pH 7, particularly the large proton coupling of the out-of-plane proton, underline that the type of radical is an OH-addition radical at position C5. Thus, a direct attack of the aromatic imidazole ring by an OH* radical from the Fenton system seems more favorable.

Histidine radicals as studied here under oxidative conditions in protein-free systems, may also be of interest in biological systems. The presented electronic structures of neutral and cationic histidine radicals may be helpful for identifying protein-associated histidine radicals.

Neutral histidine OH-addition radicals, as studied here, which are formed by oxidative attack of OH* radicals on histidine, may occur upon oxidative stress in cells under physiological conditions; at pathological misfunction (undesired Fenton reaction with free Fe^{2+}); and following radiation damage caused by UV light or X-rays.

Conclusions

Using improved EPR continuous-flow techniques, we elucidated the electronic structure of a transient histidine radical in aqueous solution at neutral pH upon Fenton oxidation of histidine. Isotropic hfcc's from EPR measurements and DFT calculations of hfcc's on an appropriate model radical collectively reveal that a neutral histidine radical is formed by OH addition to the C5 carbon of the imidazole ring. Experimental hfcc's of the imidazole ring protons, ring nitrogens, and β-protons are in excellent agreement with corresponding theoretical values from DFT calculations. A comparison of the neutral histidine radical with the cationic histidine radical (studied by the same technique[1]) shows that both types of radicals are formed by addition of an OH radical from the Fenton

system to position C5. Spin densities, however, are significantly different in the cationic and in the neutral histidine radical, particularly at the C2 and C5 carbon positions.

Acknowledgment. The authors thank the Deutsche Forschungsgemeinschaft (Project La 751/2-1), the Fonds der Chemischen Industrie (G.L. and W.L.), and the Swedish Natural Sciences Research Council (NFR) for financial support (L.A.E.). The Center for Parallel Computing (PDC) in Stockholm is gratefully acknowledged for grants of computing time.

References and Notes

(1) Lassmann, G.; Eriksson, L. A.; Himo, F.; Lendzian, F.; Lubitz, W. *J. Phys. Chem. A* **1999**, *103*, 1283.

(2) Sjöberg, B. M.; Reichard, P.; Gräslund, A.; Ehrenberg, A. *J. Biol. Chem*. **1978**, *253*, 6863.

(3) Dietz, R.; Nastaincyk, W.; Ruf, H. H. *Eur. J. Biochem*. **1988**, *171*, 321.

(4) Berry, B. A. *Photochem. Photobiol*. **1993**, *57*, 179.

(5) Whittaker, M. M.; Whittaker, J. W. *J. Biol. Chem.* **1990**, *265*, 9610.

(6) Kim, S.; Sancar, A.; Essenmacher, C.; Babcock, G. T. *Proc. Natl. Acad. Sci. U.S.A.* **1993**, *90*, 8023.

(7) Huyett, J. E.; Doan, P. E.; Gurbiel, R.; Houseman, A. L. P.; Sivaraja, M.; Goodin, D. B.; Hoffmann, B. M. *J. Am. Chem. Soc*. **1995**, *117*, 9033.

(8) Lendzian, F.; Sahlin, M.; MacMillan, F.; Bittl, R.; Fiege, R.; Pötsch, S.; Sjöberg, B.-M.; Gräslund, A.; Lubitz, W.; Lassmann, G. *J. Am. Chem. Soc*. **1996**, *118*, 8111.

(9) Pötsch, S.; Lendzian, F.; Ingemarson, R.; Hörnberg, A.; Thelander, L.; Lubitz, W.; Lassmann, G.; Gräslund, A. *J. Biol. Chem.* **1999**, *274*, 17696.

(10) Paul, H.; Fischer, H. *Ber. Bunsen-Ges. Phys. Chem.* **1969**, *73*, 972.

(11) Armstrong, W. A.; Humphreys, W. G. *Can. J. Chem.* **1967**, *45*, 2589.

(12) Fiege, R. Dissertation, Technical University of Berlin, 1997.

(13) Hellwege, K. H. *Landolt-Börnstein: Numerical Data and Functional Relationships in Science and Technology*, Group II, Vol. 9, Part a, *Magnetic Properties of Free Radicals*; Springer-Verlag: New York, 1977; pp 301−302.

(14) Waters, E. L.; Maki, A. H. *Phys. Rev.* **1962**, *125*, 233.

(15) McGarvey, B. R. *J. Chem. Phys*. **1963**, *38*, 388.

(16) Fujiwara, S.; Nagashima, K.; Codell, M. *Bull. Chem. Soc. Jpn.* **1964**, *37*, 773. Watanabe, T.; Fujiwara, S. *J. Magn. Reson.* **1970**, *2*, 103.

(17) Fischer, H. *Ber. Bunsen-Ges. Phys. Chem.* **1967**, *71*, 685.

(18) Becke, A. D. *J. Chem. Phys.* **1993**, *98*, 5648. Lee, C.; Yang, W.; Parr, R. G. *Phys. Rev.* **1988**, *B37*, 785. Devlin, P. J.; Chablowski, C. F.; Frisch, M. J. *J. Phys. Chem.* **1994**, *98* (8), 11623.

(19) McLean, A. D.; Chandler, G. S. *J. Chem. Phys.* **1980**, *72*, 5639. Frisch, M. J.; Binkley, J. S.; Pople, J. A. *J. Chem. Phys.* **1984**, *80*, 3265.

(20) Miertus, S.; Scrocco, E.; Tomasi, J. *Chem. Phys.* **1981**, *55*, 117.

(21) Barone, V.; Cossi, M.; Tomasi, J. *J. Comput. Chem.* **1998**, *19*, 404.

(22) Cances, M. T.; Mennucci, V.; Tomasi, J. *J. Chem. Phys.* **1997**, *107*, 3032.

(23) Barone, V. *Chem. Phys. Lett.* **1996**, *262*, 201. Jolibois, F.; Cadet, J.; Barone, V. *J. Am. Chem. Soc.* **1998**, *120*, 1864.

(24) Eriksson, L. A. *Mol. Phys.* **1997**, *91*, 827. Eriksson, L. A.; Himo, F.; Siegbahn, P. E. M.; Babcock, G. T. *J. Phys. Chem. A* **1997**, *101*, 9496. Wetmore, S. D.; Boyd, R. J.; Eriksson, L. A. *J. Phys. Chem. B* **1998**, *102*, 5369.

(25) Llano, J.; Eriksson, L. A. *J. Phys. Chem. B* **1999**, *103*, 5598.

(26) Frisch, M. J.; Trucks, G. W.; Schlegel, H. B.; Scuseria, G. E.; Robb, M. A.; Cheeseman, J. R.; Zakrzewski, V. G.; Montgomery, J. A., Jr.; Stratmann, R. E.; Burant, J. C.; Dapprich, S.; Millam, J. M.; Daniels, A. D.; Kudin, K. N.; Strain, M. C.; Farkas, O.; Tomasi, J.; Barone, V.; Cossi, M.; Cammi, R.; Mennucci, B.; Pomelli, C.; Adamo, C.; Clifford, S.; Ochterski, J.; Petersson, G. A.; Ayala, P. Y.; Cui, Q.; Morokuma, K.; Malick, D. K.; Rabuck, A. D.; Raghavachari, K.; Foresman, J. B.; Cioslowski, J.; Ortiz, J. V.; Stefanov, B. B.; Liu, G.; Liashenko, A.; Piskorz, P.; Komaromi, I.; Gomperts, R.; Martin, R. L.; Fox, D. J.; Keith, T.; Al-Laham, M. A.; Peng, C. Y.; Nanayakkara, A.; Gonzalez, C.; Challacombe, M.; Gill, P. M. W.; Johnson, G.; Chen, W.; Wong, M. W.; Andres, J. L.; Gonzalez, C.; Head-Gordon, M.; Replogle, E. A.; Pople, J. A., *GAUSSIAN98*, *Revision A.6*; Gaussian, Inc.: Pittsburgh, PA, 1998.

(27) Rao, P. S.; Simic, M.; Hayon, E. *J. Phys. Chem*. **1975**, *79*, 1260.

(28) Sealy, R. C.; Harman, L.; West, P. R.; Mason, R. P. *J. Am. Chem. Soc.* **1985**, *107*, 3401.

(29) Gilbert, B. C.; Larkin, J. P.; Norman, R. O. C. *J. Chem. Soc., Perkin Trans. 2*, **1972**, 1272.

(30) Samuni, A.; Neta, P. *J. Phys. Chem*. **1973**, *77*, 1629.

(31) Wertz, J. G.; Bolton, J. R. *Electron Spin Resonance*; Chapman & Hall: New York, 1986.

(32) Hellwege, K. H. *Landolt-Börnstein: Numerical Data and Functional Relationships in Science and Technology*, Group II, Vol. 9, Part c2, *Magnetic Properties of Free Radicals*; Springer-Verlag: New York, 1979; pp 8−25.

(33) Norman, R. O. C.; West, P. R. *J. Chem. Soc. B* **1969**, 389.